



Gain-of-function mutant of angiotensin II receptor, type 1A, causes hypertension and cardiovascular fibrosis in mice

Sandrine Billet,¹ Sabine Bardin,¹ Sonia Verp,¹ Véronique Baudrie,² Annie Michaud,³ Sophie Conchon,¹ Martine Muffat-Joly,⁴ Brigitte Escoubet,^{4,5} Evelyne Souil,¹ Ghislaine Hamard,¹ Kenneth E. Bernstein,⁶ Jean Marie Gasc,³ Jean-Luc Elghozi,² Pierre Corvol,³ and Eric Clauser¹

¹Institut Cochin, Université Paris Descartes, CNRS UMR 8104, INSERM U567, Paris, France. ²Faculté de Médecine Paris Descartes, INSERM U652, Université Paris Descartes, Paris, France. ³INSERM U36, Collège de France, Paris, France. ⁴INSERM IFR02, Centre d'Explorations Fonctionnelles Intégrées, Université Denis Diderot, Paris, France. ⁵INSERM U772, Collège de France, Assistance Publique Hôpitaux de Paris, Hôpital Bichat-Claude Bernard, Paris, France. ⁶Department of Pathology and Laboratory Medicine, Emory University School of Medicine, Atlanta, Georgia, USA.

The role of the renin-angiotensin system has been investigated by overexpression or inactivation of its different genes in animals. However, there is no data concerning the effect of the constitutive activation of any component of the system. A knockin mouse model has been constructed with a gain-of-function mutant of the Ang II receptor, type 1A (AT_{1A}), associating a constitutively activating mutation (N111S) with a C-terminal deletion, which impairs receptor internalization and desensitization. In vivo consequences of this mutant receptor expression in homozygous mice recapitulate its in vitro characteristics: the pressor response is more sensitive to Ang II and longer lasting. These mice present with a moderate (~20 mmHg) and stable increase in BP. They also develop early and progressive renal fibrosis and cardiac fibrosis and diastolic dysfunction. However, there was no overt cardiac hypertrophy. The hormonal parameters (low-renin and inappropriately normal aldosterone productions) mimic those of low-renin human hypertension. This new model reveals that a constitutive activation of AT_{1A} leads to cardiac and renal fibrosis in spite of a modest effect on BP and will be useful for investigating the role of Ang II in target organs in a model similar to some forms of human hypertension.

Introduction

The Ang II receptor, type 1 (AT₁), is a G protein-coupled receptor (GPCR) that transduces the main physiological actions of the renin-angiotensin system (RAS) in target cells. The major signaling events following agonist binding to this receptor are activation of phospholipase C via a Gq protein, mobilization of the calcium intracellular stores, and activation of protein kinase C. MAP kinase and Jak/STAT pathways are also activated and may participate in the hypertrophic actions of Ang II (1). There are 2 AT₁ subtypes in rodents, AT_{1A} and AT_{1B} (2, 3); the tissue distribution of the 2 subtypes (4) and knockout experiments in mice (5–7) indicate that cardiovascular, renal, and adrenal actions of Ang II are mainly mediated by AT_{1A}. The unambiguous role of AT₁ in controlling BP is evidenced in numerous animal models. For example, the knockout of AT_{1A} in mouse reduces BP (5, 6), and its overexpression by gene duplication increases BP in female mice (8). This role contrasts with the absence of clear involvement of renin angiotensin genes in genetic forms of human hypertension (9).

The concept of constitutive activation is an important breakthrough in the understanding of GPCR molecular functions: point mutations stabilize the receptor in an active conformation independent of ligand, resulting in a permanent activation of the

signaling pathways (10). Several human genetic diseases appear to be consequences of such GPCR gain-of-function mutant expression (11, 12). Therefore, it was logical to investigate whether cases of human hypertension are associated with such activating mutations of AT₁. However, no mutation of AT₁ coding sequence had previously been identified in hypertension or, more particularly, in primary hyperaldosteronism (13, 14). This absence of clearly identified gain-of-function mutations of AT₁ in humans prompted us to map the mutations of the rat AT_{1A} that cause constitutive activity by screening a randomly mutated library of the receptor with a functional assay (15). The next step was to develop an animal model expressing a gain-of-function mutant of AT₁, to answer 2 questions: (a) What are the effects of a permanent activation of this GPCR on BP? (b) If BP increases, what are the characteristics of this new experimental hypertension in terms of severity, course, target organ damage, and how or when the RAS is reset?

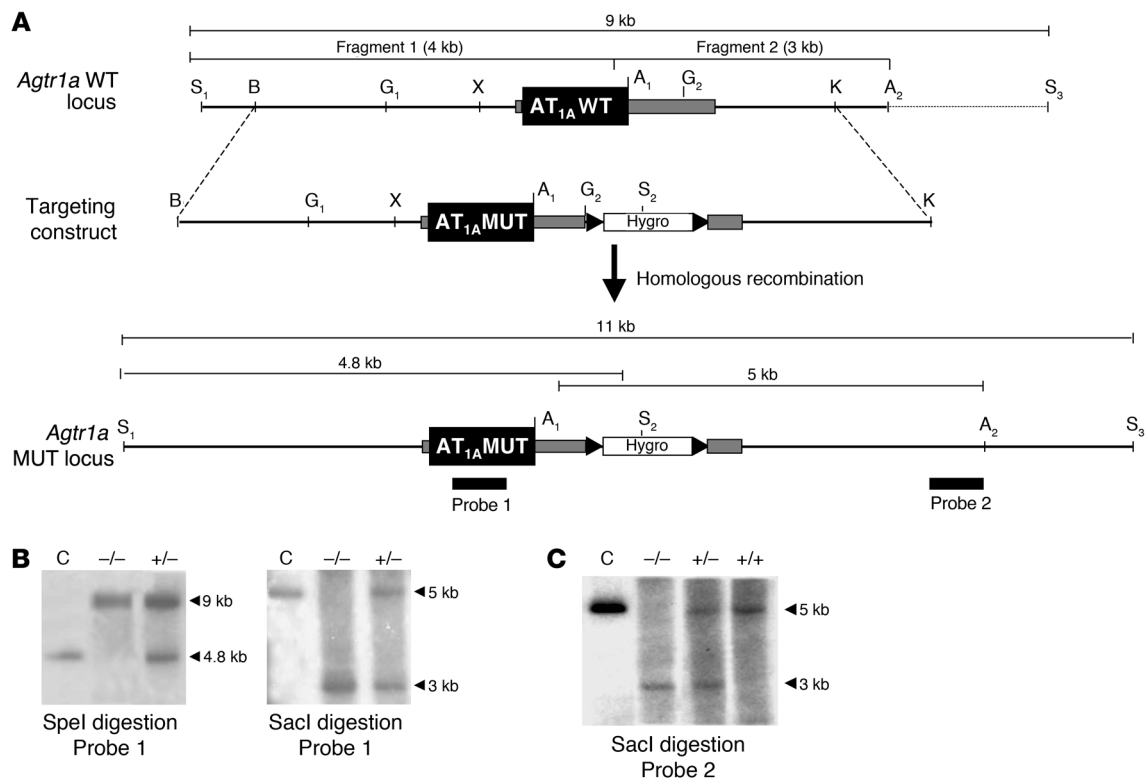
The choice of the mutation(s) was directed by the initial in vitro characterization of these constitutively activated mutants. All these AT_{1A} mutants are slightly constitutively active when compared with the WT receptor but are far from being fully active. Therefore, they can still be activated by agonists. Among the different constitutively active mutations, one of the most active is the N111S mutation. This N111S mutation, as other constitutively active mutations, induces constitutive internalization, resulting in intracellular sequestration of most receptor molecules (16).

For these reasons, we expected a mild phenotype and added to the N111S mutation a C-terminal deletion of the receptor, which impairs phosphorylation and internalization, abolishing desensitization and inducing hyper-reactivity to Ang II (17). As expected,

Nonstandard abbreviations used: ANF, atrial natriuretic factor; AT_{1A}, Ang II receptor, type 1A; AT_{1A}MUT, AT_{1A} mutant; AT_{1A}WT, AT_{1A} wild-type; AUC, area under the curve; BNP, brain natriuretic peptide; GPCR, G protein-coupled receptor; PAII, plasminogen activator inhibitor type 1; RAS, renin-angiotensin system.

Conflict of interest: The authors have declared that no conflict of interest exists.

Citation for this article: *J. Clin. Invest.* 117:1914–1925 (2007). doi:10.1172/JCI28764.

**Figure 1**

Targeted knockin of the *Agtr1a* gene by homologous recombination into ES cells and mouse. (A) Schematic representation of the targeting vector and partial restriction map of the *Agtr1a* gene locus before and after homologous recombination. The top line shows the structure of $AT_{1A}WT$ locus containing exon 3 of the gene with coding sequence (black box) and the 5' and 3' untranslated sequences (gray boxes). Exon 3 is flanked by 3 kb of intron 2 (upstream) and 2 kb of noncoding sequence (downstream). The targeting construct containing $AT_{1A}MUT$ and a hygromycin cassette (hygro) was used to replace the WT BamHI (B) KpnI (K) fragment within AT_{1A} locus (middle line). The lower line shows the targeted AT_{1A} locus with the internal probe (probe 1) and 3' external probe (probe 2) used for Southern blot analysis. (B) Southern blot analysis of targeted ES cell DNA using internal probe 1 with *SpeI* digestion (left) and using probe 2 with *SacI* digestion (right). C, control (targeting construct). $-/-$, WT cells; $+/-$, heterozygous recombinant cells. (C) Southern blot analysis of tail DNA samples from F_2 offspring (generated by crossing heterozygous mice from the first generation [F_1 mice]) digested with *SacI* and probed with the 3' external probe (probe 2). $-/-$, WT mice; $+/-$, heterozygous transgenic mice; $+/+$, homozygous transgenic mice; S, *SpeI*; B, *BamHI*; G, *BglIII*; X, *XbaI*; A, *SacI*; K, *KpnI*; N, *NotI*; E, *EcoRI*.

cellular expression of AT_{1A} bearing both these gain-of-function mutations revealed additivity of constitutive activity and hyper-reactivity to Ang II *in vitro* (18).

Here, we describe *in vivo* expression of this gain-of-function mutant in a knockin mouse model and the main characteristics of the phenotype. The constitutive activation of this receptor, associated with impaired internalization, produces a new model of mouse hypertension characterized by normal aldosterone production in the presence of very low plasma renin and the existence of cardiac, vascular, and renal fibrosis.

Results

Generation of mice expressing the $AT_{1A}N111S/\Delta329$ mutant

Homozygous mice expressing the gain-of-function AT_{1A} mutant were generated as described in Figure 1. Specific expression of the $AT_{1A}N111S/\Delta329$ mutation ($AT_{1A}MUT$), but not $AT_{1A}WT$, was identified by RT-PCR in the major AT_{1A} -expressing tissues (liver, heart, kidney, adrenal gland, and aorta) of homozygous mutant mice (data not shown). No difference in expression of AT_{1A} , AT_{1B} , or AT_2 was observed when RNA from those Ang II target tissues of

WT and mutant mice were compared using quantitative RT-PCR (Figure 2). Similar results were obtained by *in situ* hybridization using specific probes for the 3 Ang II receptors (data not shown).

All the phenotypic comparisons were made between homozygous mutant mice and WT littermates at the same age. The mutant mice had significantly lower body weights (10% to 20% lower), first observed in young animals (1 to 3 months old) and persisting throughout the life of the mouse without any clear sex difference (Table 1). An interesting and unexpected phenotypic trait was the higher concentration of red blood cells (17% higher) and hemoglobin (12% higher) and an increased hematocrit (12% higher), in mutant compared with control mice. These differences seem to correspond to true polyglobulia rather than to hemoconcentration because total plasma protein concentration and osmolality were unaffected (Table 2).

Gain-of-function features of $AT_{1A}MUT$ in mice

In vitro characterization in tissues and isolated hepatocytes. The constitutive activity of $AT_{1A}MUT$ was first investigated by comparing the phosphorylated state of signaling molecules such as STAT1, STAT3, and ERK1/2 in tissues (liver, heart, and kidney) of $AT_{1A}WT$

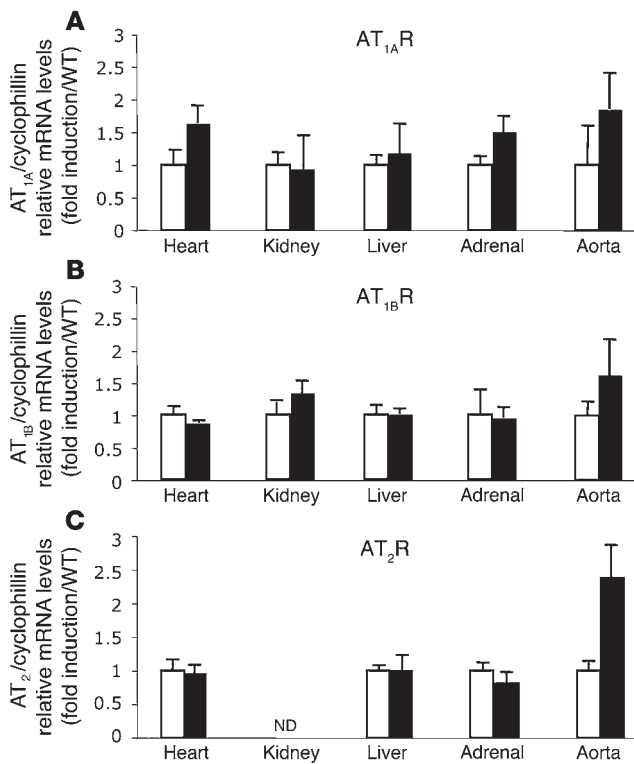


Figure 2

Quantitative RT-PCR of the Ang II receptors in target tissues. RNA from liver, kidney, heart, adrenal gland, and aorta were retrotranscribed and amplified for AT_{1A} (A), AT_{1B} (B), and AT₂ (C) mRNAs using the Light-Cycler technology in AT_{1A}WT (white bars) and AT_{1A}MUT (black bars) mice. Results are expressed in arbitrary units relative to the expression of cyclophilin gene in the same tissues. ND, not detectable.

and AT_{1A}MUT mice. Given the modest constitutive activity of the N111S/Δ329 mutant, it was not surprising to observe only modest changes in basal phosphorylations. In the liver, STAT1 increased 36% ($P = \text{NS}$) and STAT3 increased 63% ($P < 0.05$), but ERK1/2 phosphorylation did not increase, in AT_{1A}MUT mice (Figure 3A). In heart and kidney, no change was observed in STAT1 or STAT3 phosphorylation, whereas ERK1/2 basal phosphorylation was slightly (35% to 45%) but significantly increased in AT_{1A}MUT mice (data not shown). In order to gain more insight into the functional properties of AT_{1A}WT and AT_{1A}MUT receptors, their pharmacology and signaling were investigated in freshly isolated hepatocytes (Table 3 and Figure 3). The AT_{1A}MUT and AT_{1A}WT receptors presented similar expression levels and a similar affinity for Ang II in the liver. The pharmacological profiles of the AT_{1A}MUT and AT_{1A}WT receptors in the liver were compared: there were no differences in affinity for the peptide analog [Sar1-Ile8] Ang II, but AT_{1A}MUT had a lower affinity for the nonpeptide AT₁ antagonist losartan and a higher affinity for CGP42112A (a pseudopeptide agonist for AT₂) and Ang IV (angiotensins 3–8) (Table 3). Ang IV is a full agonist for these constitutively activated receptors, as indicated by the strong and dose-dependent stimulation of ERK1/2 phosphorylation (Figure 3C). This constitutive activation of AT_{1A}MUT in hepatocytes is associated with its hyperactivity and hypersensitivity to Ang II: compared with the AT_{1A}WT receptor, the maximal ERK1/2 phosphorylation in the AT_{1A}MUT receptor increased by 2-fold and sensitivity of the response to Ang II was better (50% effective concentration [EC₅₀] = 0.39 ± 0.16 nM, AT_{1A}MUT; 2.10 ± 0.55 nM, AT_{1A}WT; $P < 0.05$) (Figure 3B). This pharmacological and signaling profile

is similar to that reported for the same mutant in transfected cells (18) and reproduces some of the characteristics of constitutively activated AT₁, which bind inverse agonists with at least 100-fold lower affinity compared with AT_{1A}WT receptors (19). Conversely, CGP42112A and Ang IV have a much better affinity and become full agonists for AT_{1A}MUT (15).

In vivo vascular responsiveness to Ang II. The BP response to Ang II was analyzed by invasive methods on anesthetized 5-month-old animals (Figure 4). As expected, Ang II increased the BP of AT_{1A}WT animals in a dose-dependent manner, with a sharp initial peak after injection followed by a progressive return to basal BP within approximately 3 minutes (Figure 4A). Interestingly, in AT_{1A}MUT mice, the initial BP rise was followed by a plateau that lasted for at least 30 minutes, without any return to the basal level (Figure 4A). The cumulative doses of Ang II (0.0001–30 μg/kg) raised the systolic BP measured 10 minutes after the last injection by 60 mmHg in AT_{1A}MUT mice, whereas it increased only 25 mmHg in AT_{1A}WT animals. The BP response to Ang II as assessed from the area under the curve in AT_{1A}MUT mice (ED₅₀ = 0.07 ± 0.16 μg/kg) was considerably more sensitive than that in the AT_{1A}WT mice (ED₅₀ = 0.63 ± 0.23 mg/kg; $P < 0.05$) (Figure 4B). These data suggest strongly that the transduction of the BP response to Ang II via the AT_{1A}MUT receptor is more sensitive compared with AT_{1A}WT and that this response is not desensitized. This nondesensitized BP response is independent of kidney AT_{1A}, at least in acute conditions, since binephrectomy does not modify the sustained BP response to Ang II (data not shown). In addition, the specificity of the sustained BP response via AT_{1A}MUT is assessed by the clear agonist effect of CGP42112A, which is ineffective in AT_{1A}WT mice (Figure 4C) and by a similar BP response to epinephrine in the 2 groups of mice (data not shown).

AT_{1A}MUT mice are hypertensive

Tail-cuff measurements of systolic BP (Figure 5A) revealed a BP increase in AT_{1A}MUT mice as young as 5 weeks old. This BP

Table 1
General physiological parameters of AT_{1A}WT and AT_{1A}MUT mice

Parameter	Age (mo)	Sex	AT _{1A} WT	n	AT _{1A} MUT	n
BW (g)	1–3	M	26.8 ± 1.1	6	22.0 ± 1.4 ^A	5
	5–7	M	33.3 ± 1.2	3	28.7 ± 2.3 ^A	3
	5–7	F	26.2 ± 0.9	5	20.9 ± 0.4 ^A	5
	7–11	M	34.3 ± 0.7	10	30.7 ± 0.7 ^B	10
	7–11	F	29.3 ± 0.4	9	26.5 ± 0.4 ^B	13
	12–15	M	38.2 ± 2.2	3	33.5 ± 0.8 ^A	3
	12–15	F	27.8 ± 1.0	6	24.6 ± 0.7 ^A	6
Food intake (g)	5–7	M+F	3.71 ± 0.27	8	3.62 ± 0.32	8
Water intake (ml)	5–7	M+F	3.43 ± 0.22	8	3.17 ± 0.44 ^A	8
Diuresis (ml)	5–7	M+F	1.50 ± 0.11	8	1.09 ± 0.13 ^A	8

^A $P < 0.05$, ^B $P < 0.01$ compared with AT_{1A}WT. BW, body weight.



Table 2
Physiological parameters of AT_{1A}WT and AT_{1A}MUT mice

Parameter	Age (mo)	Sex	AT _{1A} WT	n	AT _{1A} MUT	n
Blood Fasting glycemia (mg/dl)	7–11	M+F	84.1 ± 1.1	19	79.7 ± 1.5	23
Ht (%)	6.5–9	M+F	36.6 ± 1.4	10	41.1 ± 1.2 ^A	10
rbc (10 ⁶ /μl)	6.5–9	M+F	7.6 ± 0.2	10	8.9 ± 0.3 ^B	10
Hb (g/dl)	6.5–9	M+F	12.5 ± 0.4	10	14.1 ± 0.4 ^A	10
Total plasma proteins (g/l)	6.5–9	M+F	37.9 ± 1.7	8	38.7 ± 2.4	7
Osmolality (mOsm/kg H ₂ O)	6.5–9	M+F	254 ± 10	9	252 ± 12	9
Na ⁺ (mmol/l)	6.5–8	M+F	147 ± 2	5	145 ± 2	6
K ⁺ (mmol/l)	6.5–8	M+F	5.0 ± 0.2	5	5.8 ± 0.8	6
Creatinine (μmol/l)	6.5–9	M+F	23.5 ± 1.7	8	22.7 ± 0.8	7
Urea (mmol/l)	6.5–9	M+F	7.1 ± 0.5	8	8.7 ± 0.4 ^A	7
Urine Osmolality (mOsm/kg H ₂ O)	5–7	M+F	2044 ± 101	7	2504 ± 166 ^A	8
Na ⁺ (μmol/d)	5–7	M+F	324 ± 26	8	262 ± 29	8
K ⁺ (μmol/d)	5–7	M+F	433 ± 33	8	333 ± 31 ^A	8
Creatinine (nmol/d)	5–7	M+F	8243 ± 506	8	5651 ± 480 ^C	8
Urea (mmol/d)	5–7	M+F	1946 ± 156	6	1386 ± 190 ^A	7
Microalbumin (μg/d)	5–7	M+F	11.1 ± 1.3	8	12.32 ± 1.80	8

^AP < 0.05, ^BP < 0.01, ^CP < 0.001 compared with AT_{1A}WT. Ht, hematocrit; Hb, hemoglobin.

elevation was moderate (~20 mmHg) and persisted with similar severity throughout life without progressive aggravation. It was more severe in male mice (23–35 mmHg) than in female mice (11–17 mmHg) mice. Malignant hypertension was not detected at any time, despite careful testing for symptoms. This permanent hypertension was confirmed by invasive measurements of systolic (122 ± 4 mmHg in AT_{1A}MUT mice compared with 95 ± 6 mmHg in AT_{1A}WT mice; P < 0.01) and diastolic BP values (92 ± 6 mmHg in AT_{1A}MUT mice compared with 69 ± 5 mmHg in AT_{1A}WT mice; P < 0.01) in anesthetized animals.

Pharmacological reduction of BP by AT₁ blockers (ARBs) was investigated, despite the fact that ARBs (inverse agonists) present altered affinities for AT_{1A} constitutively activated mutants (19). According to Le et al. (19), candesartan has the highest ARB affinity for the N111S mutant (K_d = 2.49 ± 0.29 nM compared with 0.27 ± 0.07 for the AT_{1A}WT receptor) and losartan has the lowest affinity for the mutant receptor (K_i = 548 ± 140 nM). Candesartan treatment (10 mg/kg/d) during 25 days reduced (by approximately 30 mmHg) BP of AT_{1A}MUT animals to normal levels (Figure 5B). However, losartan treatment (30 mg/kg/d or 150 mg/kg/d) for 2 weeks significantly reduced the BP of AT_{1A}WT animals (by 11 mmHg and 20 mmHg for the respective doses) but had no effect on AT_{1A}MUT animals (data not shown).

AT_{1A}MUT mice have high BP with low-renin hypertension and relative hyperaldosteronism

The consequences for the RAS of the expression of this AT_{1A}MUT in mice were analyzed. Plasma renin concentration (PRC) was considerably lower in mutant mice than in AT_{1A}WT mice (Figure 6A). This low PRC level was presumably the consequence of a large decrease in the production of renin by the juxtaglomerular apparatus in the kidney. This was confirmed by *in situ* hybridization for renin mRNA in these structures for both adult (5-month) and neonate (2-day) mice (Figure 6, C and D). Plasma renin substrate was unaffected (data not shown). These low-renin concentrations in AT_{1A}MUT mice resulted in

a 50% decrease of immunoreactive angiotensin plasma concentrations (Figure 6B). Further studies are needed to identify whether this decrease involves Ang II, Ang III, and Ang IV equally, as they are all measured by this assay. The low-renin production contrasts with normal concentrations of aldosterone in both plasma and urine from AT_{1A}MUT animals (Figure 6E). No morphological abnormality was observed in the adrenal cortex of AT_{1A}MUT animals. There was no hypertrophy of the zona glomerulosa, and the aldosterone synthase gene (CYP11B2) was expressed at a normal level, as assessed by *in situ* hybridization (data not shown). A 10-fold increase in plasma aldosterone/renin ratio was the main hallmark of the endocrine profile of this new experimental hypertension (Figure 6F).

Renal consequences of hypertension and RAS alterations

We investigated the pathophysiological consequences of the expression of AT_{1A}MUT on kidney structure and functions: urinary samples were collected from 6- to 7-month-old animals in metabolic cages, plasma was sampled, and renal morphology was analyzed.

The 24-hour diuresis of AT_{1A}MUT animals was lower than AT_{1A}WT (Table 1). This was associated with a higher urinary osmolality but a normal plasma osmolality (Table 2).

After correction for body weight and 24-hour diuresis, creatinine excretion in mutant mice was significantly lower than in AT_{1A}WT mice (Figure 7A), whereas plasma creatinine concentration was normal and plasma urea was slightly but significantly higher (Table 2). There were no obvious tubular pathology or major plasma or urinary electrolyte abnormalities (Figure 7B and Table 2).

These moderate functional changes were associated with periglomerular and perivascular fibrosis without major changes in glomerular or tubular morphology (Figure 7C). Confirmation of this fibrosis was investigated by measuring expression of 2 molecular markers, collagen αI and plasminogen activator inhibitor type 1

Table 3
Pharmacological properties of AT_{1A}WT and AT_{1A}MUT in membranes extracted from hepatocyte cells

Experiment type	Parameter	AT _{1A} WT	AT _{1A} MUT
Saturation ^A	K _d (nM)	0.54 ± 0.03	0.58 ± 0.06
	Bmax (fmol/mg)	12.6 ± 2.4	11.0 ± 2.3
Competition ^B	K _i (nM)		
	[Sar1-Ileu8] Ang II	0.24 ± 0.21	0.41 ± 0.19
	Losartan	14.5 ± 3.9	1857.5 ± 728.2 ^C
	CGP42112A	1375.7 ± 383.5	74.8 ± 20.9 ^C
	Ang IV	207.8 ± 22.5	11.2 ± 3.5 ^C

^AParameters of [¹²⁵I]Ang II binding calculated from saturation experiments.

^BK_i calculated from competition experiments of [¹²⁵I]Ang II with the indicated compounds. Results are expressed as mean ± SEM of 3 independent experiments, in which each point was performed in triplicate. ^CP < 0.05 compared with AT_{1A}WT.

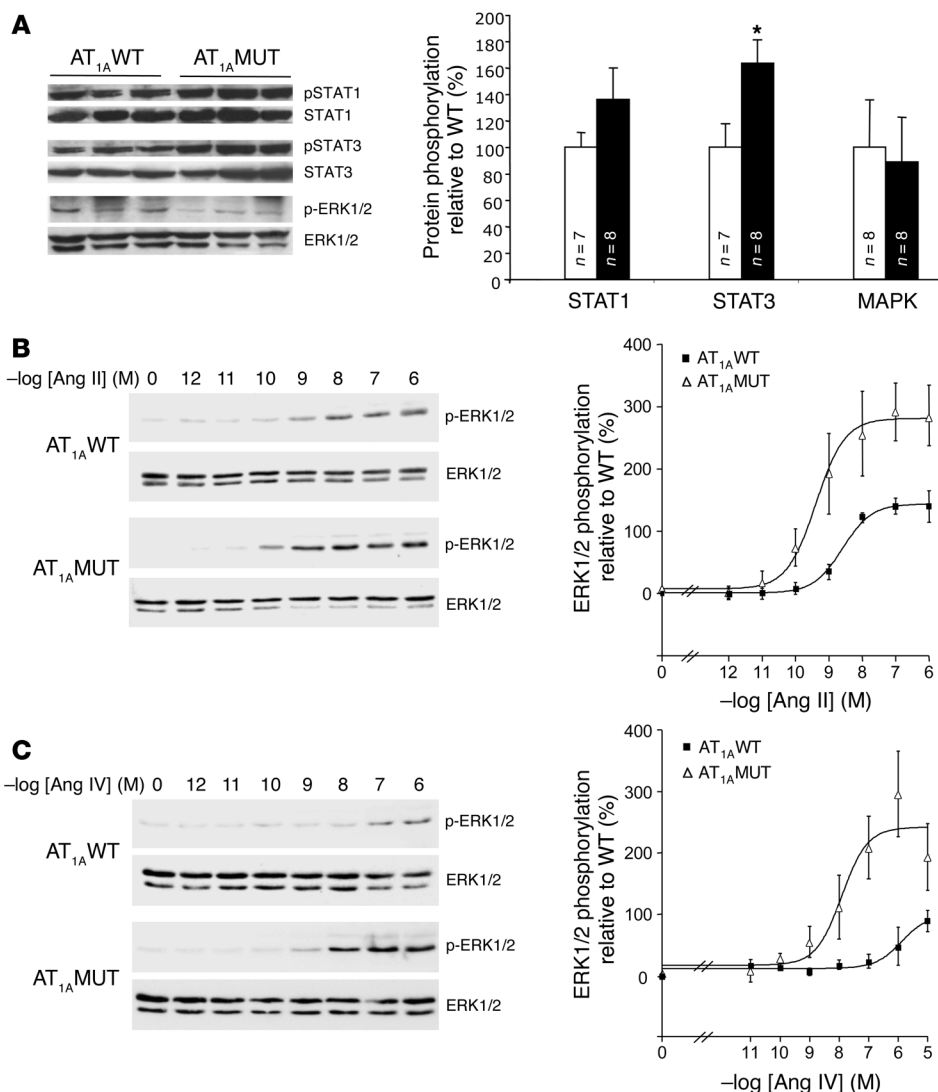


Figure 3 Signaling properties of AT_{1A} in tissues and primary hepatocyte cultures from AT_{1A}WT and AT_{1A}MUT mice. (A) Basal phosphorylation of STAT1, STAT3, and ERK1/2 in the liver. Left: Representative Western blot for 3 AT_{1A}WT and 3 AT_{1A}MUT mice. Right: Histograms show mean ± SEM of the ratio of phosphorylated protein to total protein and expressed as a percentage of this ratio in AT_{1A}WT corresponding tissue. White bars, AT_{1A}WT; black bars, AT_{1A}MUT. *P < 0.05 compared with AT_{1A}WT. (B and C) Stimulation of ERK1/2 phosphorylation by Ang II (B) and Ang IV (C). Primary cultured hepatocytes from AT_{1A}WT (black squares) and AT_{1A}MUT (white triangles) mice were serum-starved for 3 hours and stimulated with Ang II (B) or Ang IV (C) for 5 minutes at 37°C. Left panels show representative immunoblots of phosphorylated ERK1/2 (p-ERK1/2) and total ERK1/2 (ERK1/2). ERK1/2 phosphorylation was quantified by densitometry, normalized to the amount of total ERK1/2 in each lane and expressed as a percentage over basal phosphorylation of ERK1/2 as shown in the right panels. Results are mean ± SEM of 3 independent experiments.

(PAI1), using quantitative RT-PCR (Figure 7D). Despite a 3-fold increase in these markers in AT_{1A}MUT mice, this difference was not significant due to an important variability of the markers in AT_{1A}MUT mice. The origin of this variability is not linked to age but may be linked to gender, and it should be further investigated. A moderate but significant hypertrophy of the small renal arteries was also observed (Figure 8A).

AT_{1A}MUT mice present with progressive cardiac fibrosis

Morphological and echocardiographic investigations of the cardiac structure and function in 5- and 12-month-old AT_{1A}MUT and AT_{1A}WT mice were performed. The AT_{1A}MUT animals did not present any major cardiac hypertrophy. The heart weight/body weight ratio was unchanged in 5-month-old animals and in 12-month-old females (Figure 8B). However, the ratio was slightly but significantly higher in 12-month-old AT_{1A}MUT males compared with AT_{1A}WT males (data not shown). These changes in heart weight were not associated with any increase in atrial natriuretic factor (ANF) expression, but a clear (>3-fold) and significant increase of brain natriuretic peptide (BNP) expression was observed in the heart of AT_{1A}MUT mice (Figure 8C).

The absence of obvious cardiac hypertrophy in mutant mice was confirmed by echocardiography. Left ventricle mass was the same in mutant and AT_{1A}WT mice at both 5 and 12 months of age (Table 4). Echocardiography detected a mild, late decrease in contractility in AT_{1A}MUT mice as assessed by tissue Doppler imaging (Table 4); the ejection fraction was not significantly lower, but there was mild left ventricle remodeling, as shown by the higher left ventricle end-diastolic diameter relative to body weight in AT_{1A}MUT mice. However, a clear, early alteration in diastolic left ventricle relaxation was detected (Table 4) with variables associated with myocardial relaxation being abnormal. In 12-month-old mice the abnormal diastolic function was accompanied by high left ventricle filing pressure, as depicted by the ratio of the maximal blood velocity of early left ventricle inflow to the maximal velocity of early diastolic motion of the mitral annulus, with relatively conserved systolic function, the hallmark of diastolic heart failure.

Morphological analysis of serial heart slices unambiguously showed the presence of a cardiac fibrosis in AT_{1A}MUT mice (Figure 8D), without cardiomyocyte hypertrophy or inflammation. This fibrosis predominated in pericoronary area but was also observed in interstitial spaces. It was not detected until 3 months of age, but it

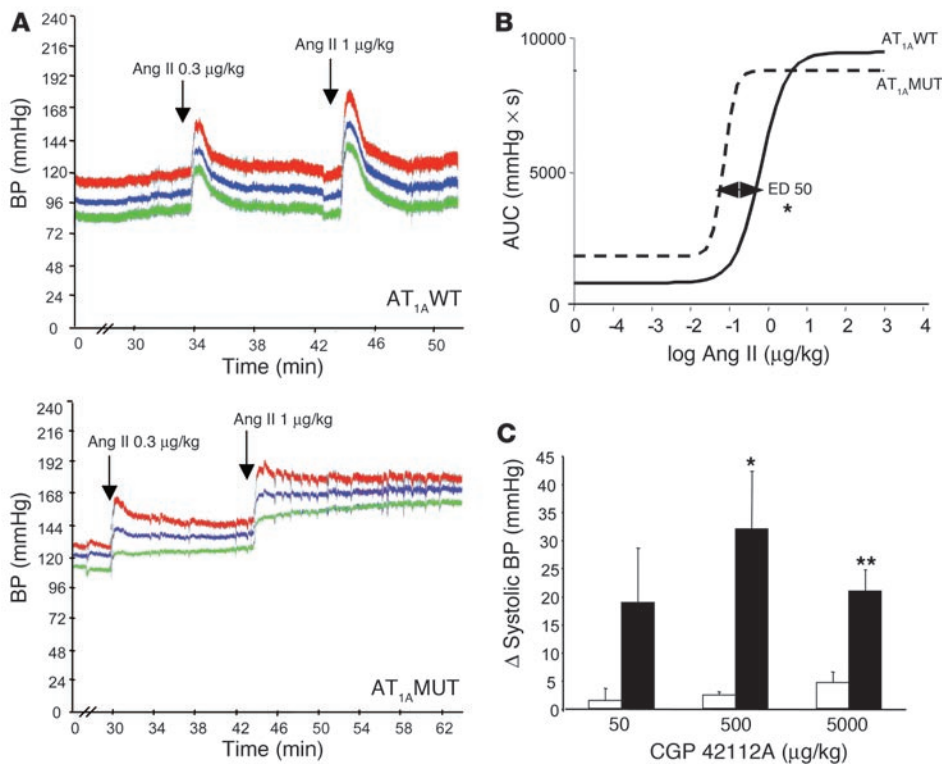


Figure 4 Pressor response to Ang II of AT_{1A}WT and AT_{1A}MUT mice. Effect of cumulative intravenous bolus doses of Ang II on BP in anesthetized mice. (A) Representative recordings, following Ang II injections (arrows), of systolic (red), mean (blue), and diastolic (green) BPs in AT_{1A}WT and AT_{1A}MUT mice. After each Ang II dose, BP stabilized at a significantly higher level in AT_{1A}MUT mice than in control mice. (B) Ang II dose-response effect on systolic BP. The area under the curve (AUC; see Methods) was measured for each Ang II dose in AT_{1A}WT (solid line) and AT_{1A}MUT mice (dotted line). (C) Systolic BP response to increasing bolus doses of CGP42112A injected in anesthetized AT_{1A}WT (white bars) and AT_{1A}MUT (black bars) mice. *P < 0.05, **P < 0.01 compared with AT_{1A}WT.

became apparent in 4-month-old mutant mice and progressed with time to become evident at 1 year without any sex preference. This cardiac fibrosis was confirmed at the molecular level, with an important (>3-fold) and significant increase of collagen αI expression, whereas only a limited and nonsignificant increase of PAI1 expression was observed in 5-month-old AT_{1A}MUT mice (Figure 8E).

Discussion

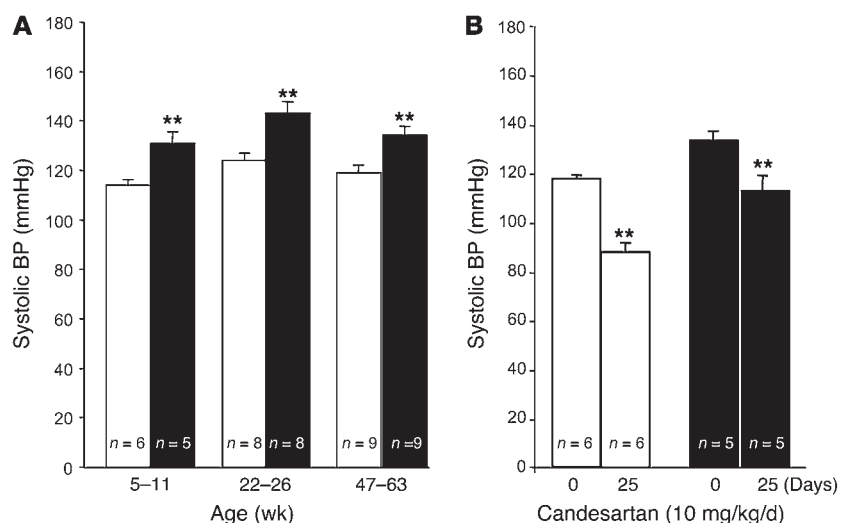
Expression of a gain-of-function AT_{1A}MUT at its physiological sites in the mouse results in a permanent, nonmalignant form of hypertension characterized by a normal aldosterone level but low-renin secretion. This permanent hypertension is unusual because of its early development, the absence of aggravation during mouse life, its moderate severity, and its predominance in males. The roles of various genes of the RAS that are potentially involved in the control of BP (renin, angiotensinogen, angiotensin-converting enzyme, and AT₁ genes) has been extensively investigated both by over-expression and by inactivation in mice and rats

(20–26). Inactivation of the *Agtr1a* gene (27) but not the *Agtr1b* (7) or the *Agtr2* (28, 29) genes, causes a BP decrease, and the duplication of *Agtr1a* gene results in a moderate increase of BP in female mice (8). Sex differences in BP changes were also observed in *Ren1d* KO (21) and *Ace* KO (20) female mice, which had decreased BP, but these apparently discordant differences were never explored further. These data confirm that quantitative alterations of RAS gene expression modulate BP. However, there are no data about the effect of constitutive activation of any of the RAS components on BP or cardiovascular or renal functions.

In the present study, the observed phenotype is a result of qualitative, not quantitative, functional alterations of AT_{1A}. Indeed,

Figure 5

Systolic BP measured by the tail-cuff method. (A) Systolic BP measured throughout the lives of AT_{1A}WT mice (white bars) and AT_{1A}MUT mice (black bars). **P < 0.01 compared with AT_{1A}WT. (B) Systolic BP measurements after candesartan treatment. Animals were treated with candesartan in drinking water (10 mg/kg/d) for 25 days. Systolic BP was measured as above on the last 3 days of the treatment period. **P < 0.01 compared with untreated animals.



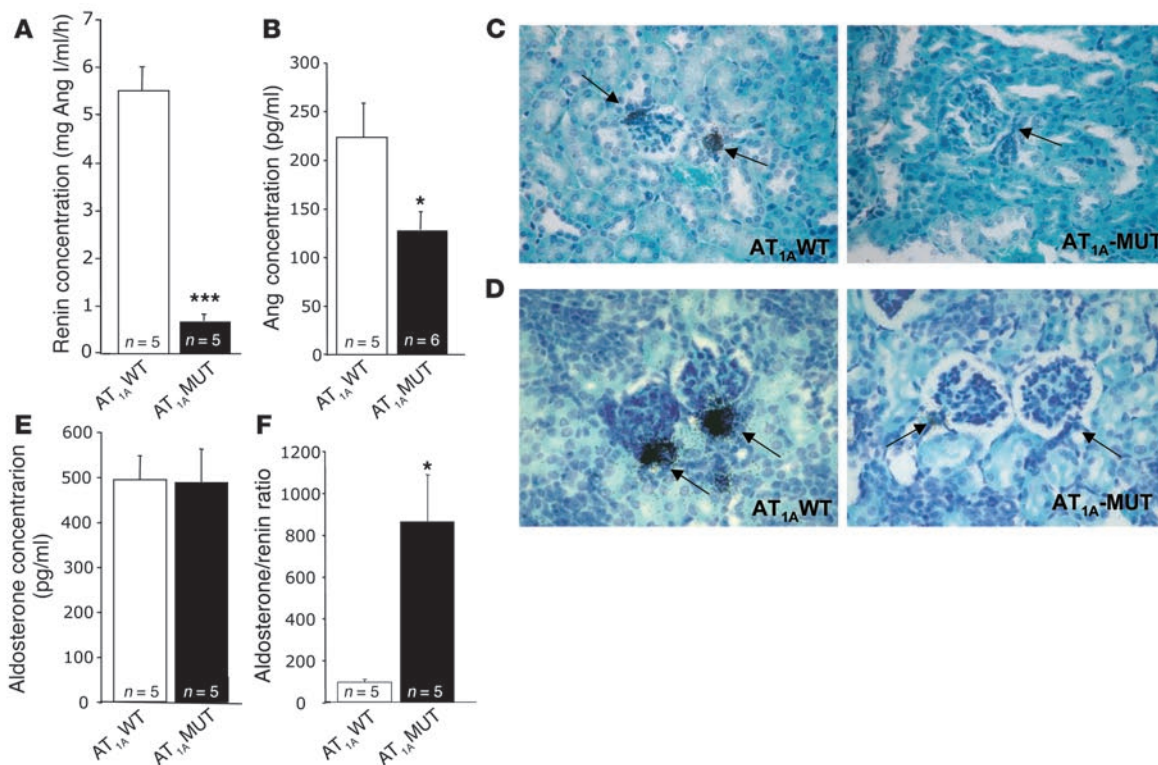


Figure 6 Renin-angiotensin-aldosterone system parameters. Plasma renin (A), plasma immunoreactive angiotensin (B), and plasma aldosterone (E) concentrations were determined in AT_{1A}WT mice (white bars) and AT_{1A}MUT mice (black bars). (C) Representative in situ hybridization detection of renin expression in kidney sections from AT_{1A}WT and AT_{1A}MUT adult (C) and neonate (D) animals. The juxtaglomerular apparatus is indicated by arrows. Relative hyperaldosteronism was also evaluated by computing the aldosterone/renin ratio (F). **P* < 0.05, ****P* < 0.001 compared with AT_{1A}WT.

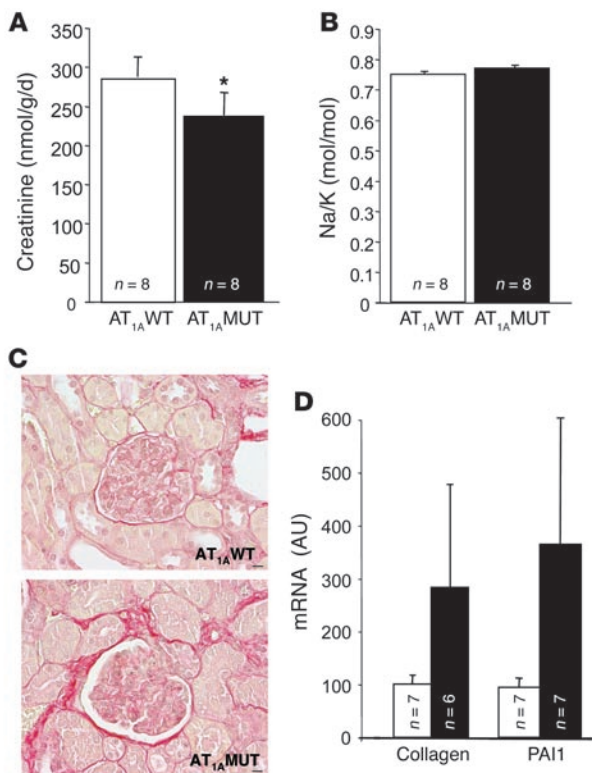
Agtr1a, *Agtr1b*, and *Agtr2* levels of expression are unchanged in mutant mouse tissues as assessed by quantitative RT-PCR in several target organs of Ang II and Ang II binding and in situ hybridization. These qualitative alterations of AT_{1A} associate 2 gain-of-function mutations.

The first mutation is an N111S point mutation that induces partial constitutive activation of AT_{1A}. Constitutive activation of AT_{1A} is confirmed in vivo in AT_{1A}MUT mice by several experimental data: (a) pharmacological and signaling profiles of AT_{1A} that are similar in hepatocytes from AT_{1A}MUT mice and cells transfected with different constitutively active AT_{1A} mutants (15, 18); (b) increase of STAT1, STAT3, and ERK1/2 basal phosphorylation in some Ang II target tissues; (c) correction of hypertension with the inverse agonist candesartan, which has high affinity for AT_{1A}MUT (19); (d) and full agonist effect of CGP42112A on AT_{1A}MUT mouse BP, as previously shown in vitro on constitutively active mutants (15).

Altogether, these results sustain the hypothesis that, at least in part, the mouse phenotype is a result of constitutive activation of the receptor. This animal model, in addition to cellular models expressing the AT_{1A}MUT receptor, could thus help in the evaluation of other new and more potent agonists or antagonists. The AT_{1A}MUT mouse is the first animal model expressing a constitutively active GPCR in a physiological context. Previous reports have described overexpression of constitutively active mutants of the α_{1B} and β₂ adrenergic receptors in the heart (30, 31) and the parathyroid hormone receptor in the growth plate (11). Surprisingly the gain-of-function phenotype was often replaced by a loss-

of-function phenotype as a result of cellular sequestration or toxicity of the GPCR mutant. To avoid constitutive internalization and desensitization of the constitutively active AT_{1A} previously described in cellular models (16), we added a second mutation, i.e., a C-terminal deletion (Δ329). In absence of the C-terminal tail, the receptor cannot be phosphorylated, does not interact with β-arrestins, is not internalized, and is not desensitized (17). The in vivo consequences of this deletion confirmed the observations in cellular systems. The hypertensive response to Ang II was amplified and long lasting in AT_{1A}MUT animals. This sustained response to Ang II strongly suggests that the mutant receptor is not turned off after Ang II activation. Other reports indicated the possibility of desensitization alterations of GPCRs such as β-adrenergic receptors in heart failure (32), but to our knowledge the present knockin (AT_{1A}MUT) is the first animal model in which the physiological consequences of the expression of a non-desensitized GPCR could be investigated.

Hypertension of AT_{1A}MUT mice is associated with low plasma renin levels, a consequence of a decreased renal renin synthesis, as shown by in situ hybridization and low plasma angiotensin levels. In contrast, there is no alteration in aldosterone synthesis, plasma and urinary aldosterone are normal, there are no major changes in electrolyte balance, and notably, there is normal kalemia. Such a discrepancy between renin production and aldosterone production has already been observed in *Agtr1a* KO mice (high renin and normal aldosterone levels) (33). A possible explanation for the lack of aldosterone overproduction is the particular status of the zona

**Figure 7**

Functional and morphological characterization of AT_{1A}WT and AT_{1A}MUT mouse kidney. Kidney function was evaluated by measuring 24-hour urinary creatinine (**A**) and Na/K balance (**B**) for 3 days. All assays were performed in AT_{1A}WT (white bars) and AT_{1A}MUT (black bars) mice fed a normal-sodium diet. (**C**) Representative kidney histological sections from both mice genotypes stained with Sirius red. Scale bars: 10 μ m. (**D**) Quantitative RT-PCR of collagen α I and PAI1 mRNA in AT_{1A}WT (white bars) and AT_{1A}MUT (black bars) kidneys. * $P < 0.05$ compared with AT_{1A}WT.

AT_{1A}MUT acts on water homeostasis mostly by urine concentration in the kidney (33).

Ang II also controls the sodium balance by regulating renal hemodynamics and stimulating sodium reabsorption in the renal tubules directly or indirectly via aldosterone secretion. No major modification of the sodium balance was detected in AT_{1A}MUT mice on a normal sodium diet, but further studies involving various sodium diets and water intakes will be necessary to precise the link between sodium balance and hypertension in these animals.

The consequences of AT_{1A} activation on end organ damage were investigated in AT_{1A}MUT mice. Cardiovascular hypertrophy, as assessed by morphological and echographical analyses, is moderate and late in mutant mice. It is observed especially in old male mice, suggesting a predominant role of hypertension in its development. Therefore, AT_{1A} activation in the heart seems to have little physiological involvement in cardiomyocyte hypertrophy. This result strongly contrasts with other experimental data, showing that AT_{1A}-specific overexpression in the heart of transgenic mice (37–39) induces massive cardiac hypertrophy with conduction defects but without hypertension. However, part of this phenotype may be the result of a nonspecific effect of AT_{1A} overexpression in cardiomyocytes.

The major cardiovascular modification in AT_{1A}MUT mice is fibrosis. This fibrosis appears in early adulthood (4 months), progresses throughout the life of the mouse, is predominantly perivascular but is also interstitial, and is associated with an increased expression of collagen α I. Cardiac fibrosis parallels the functional cardiac alterations that occur early in AT_{1A}MUT mice (5 months of age), and this phenotype is similar to that observed in human cardiac fibrotic diseases, i.e., alteration of diastolic function, with subsequent evolution toward diastolic heart failure. The results in AT_{1A}MUT mice point to a direct action of Ang II via AT_{1A} on extracellular matrix regulation in cardiovascular fibroblasts, as suggested by others (40). Further investigation of the AT_{1A}MUT model is needed to delineate the direct physiological effects of AT_{1A} activation in cardiovascular hypertrophy, fibrosis, and remodeling, independent of hypertension and other factors such as aldosterone.

In conclusion, this description of what we believe to be the first animal model expressing a gain-of-function mutation of AT_{1A} in a physiological context may provide new insight into the pathophysiology and therapy of human hypertension. Our findings suggest that such genetic defects in humans, if they exist, contribute to high aldosterone–low-renin forms of hypertension. The prevalence of these forms of hypertension, as assessed by aldosterone/renin ratio measurements, is high (34). This model also reveals the importance of AT₁ activation in cardiovascular remodeling and therefore sustains the usefulness of RAS inhibition in these disorders.

glomerulosa in the mouse adrenal cortex in terms of AT₁ expression, since these cells express equal amounts of AT_{1A} and AT_{1B} (4). Therefore, the production of aldosterone is stimulated by the gain-of-function AT_{1A} but is no longer stimulated via AT_{1B} because of the decrease in circulating Ang II. The result may be a normal aldosterone production, which is nevertheless inappropriate in view of the low-renin values. Alternatively the normal levels of aldosterone could be the result of other RAS-independent factors regulating aldosterone production. This phenotype, together with the hypersensitivity to Ang II infusion, resembles that classically described in primary hyperaldosteronism, in which there is an abnormal renin/aldosterone ratio (34). We and others have tried unsuccessfully to identify mutations of the *Agr1* gene in aldosterone-producing adenomas (13, 14), but other forms of low-renin hypertension with or without hyperaldosteronism should be screened.

This AT_{1A}MUT mouse is an interesting model in which to investigate the renal modifications that follow receptor activation. Such a model may help to define the roles of renal and extrarenal tissues in the development of hypertension. A recent, elegant study by Crowley et al. demonstrated the additive roles of kidney and systemic tissues in BP regulation using a renal cross-transplantation strategy (35). Similar experiments in AT_{1A}MUT mice would further define these distinct roles in the regulation of BP via the RAS.

Ang II regulates water balance by both central (dipsogenic effects) and renal (vasopressin secretion, urine concentration) actions. The AT_{1A}MUT mice had lower diuresis and higher urinary osmolality than controls. The opposite (higher diuresis and lower urinary osmolality) has been observed in AT_{1A} KO mice (36). Normal plasma natremia in AT_{1A}MUT mice excludes the presence of an inappropriate vasopressin secretion, and there is no clear dipsogenic effect of the mutant receptor. This suggests that

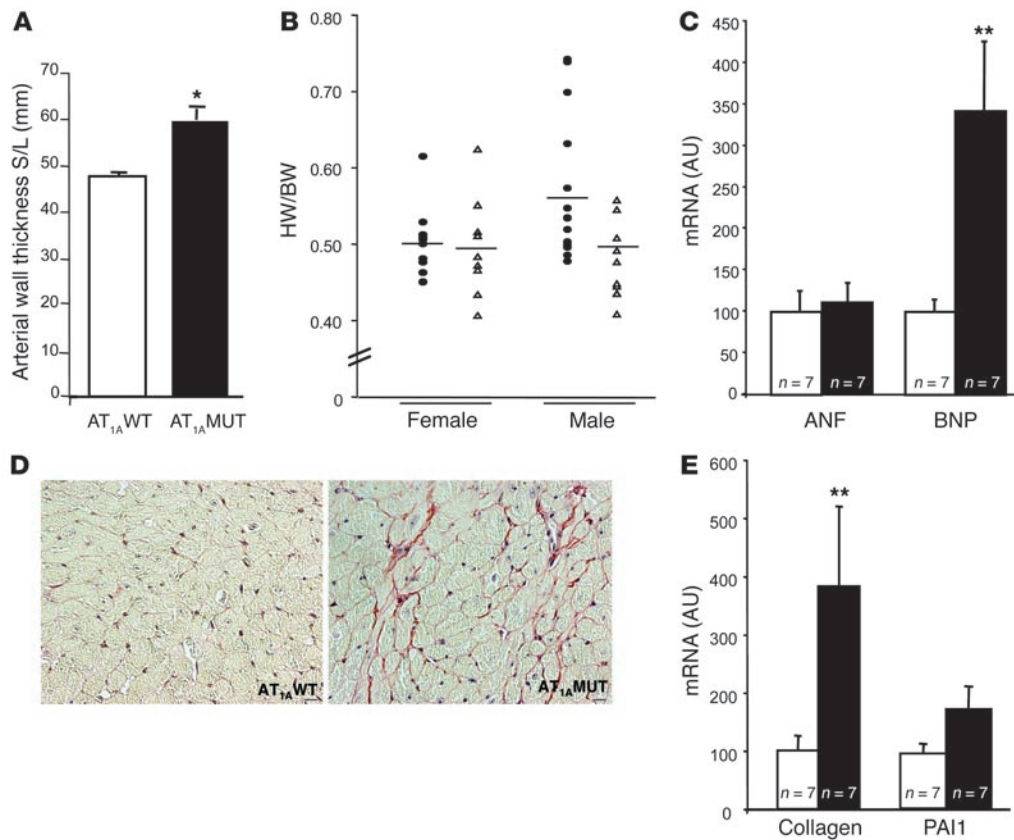


Figure 8

Cardiovascular characterization of AT_{1A}MUT and AT_{1A}WT mice. **(A)** Vascular morphology was assessed by morphometric analysis of the wall thickening ratio (S/L) in renal arteries in 5-month-old AT_{1A}WT (white bar) and AT_{1A}MUT (black bar) littermates. Three mice were studied in each group, and a mean of 20 arteries were measured in each mouse. **P* < 0.05 compared with AT_{1A}WT. **(B)** Cardiac hypertrophy was assessed by the ratio of heart weight to body weight (HW/BW) in 6- to 10-month-old AT_{1A}WT (white triangles) and AT_{1A}MUT (black circles) littermates. **(C)** Quantitative RT-PCR of ANF and BNP mRNA in AT_{1A}WT (white bars) and AT_{1A}MUT (black bars) hearts. **(D)** Myocardial sections from 5-month-old AT_{1A}WT and AT_{1A}MUT mice were stained with Sirius red. Scale bar: 10 μm. **(E)** Quantitative RT-PCR of collagen α1 and PAI1 mRNA in AT_{1A}WT (white bars) and AT_{1A}MUT (black bars) hearts. ***P* < 0.01 compared with AT_{1A}WT.

Methods

Generation of AT_{1A}MUT mice

The targeting AT_{1A}-N111S/Δ329 construct was derived from a 7-kb SpeI(S1)-SacI(A2) genomic fragment contained in a commercial BAC clone (catalog no. FBAC4432; Incyte Genomics Inc.). This 7-kb fragment contains the entire exon 3 of the mouse *Agtr1a* gene flanked with 3 kb of intron 2 at its 5' end and 2 kb of noncoding sequence at its 3' end (Figure 1). Exon 3 is composed of 5' untranslated sequence (60 bp), the entire coding sequence, and the 3' untranslated sequence (830 bp). This 7-kb fragment was digested with SacI, and 4-kb SpeI(S1)-SacI(A1) (fragment 1) and 3-kb SacI(A1)-SacI(A2) (fragment 2) were inserted into a pBlueScript vector (Figure 1A). The N111S mutation and C-terminal deletion of the AT_{1A} coding sequence were introduced into a 1.5-kb XbaI(X)-SacI(A1) fragment derived from fragment 1 by site-directed mutagenesis using sequential PCR, as previously described (18). The mutated 1.5-kb XbaI/SacI fragment was reintroduced into fragment 1 in place of the corresponding WT fragment, and fragment 2 was reintroduced into this construction at the SacI site.

The hygromycin resistance gene flanked by loxP sites was inserted into the construct at a Bgl2 site located in the 3' untranslated sequence. First, a BglIII(G1)-BglIII(G2) fragment containing the AT_{1A}MUT sequence was deleted and a linker containing unique NruI and NotI sites was inserted

into the BglIII site. The BglIII-BglIII fragment was then reintroduced in the correct orientation into the BglIII site upstream from the hygromycin cassette ligated between the NruI and NotI sites. This construct was verified by DNA sequencing and restriction mapping.

The final construct was digested with BamHI and KpnI to eliminate plasmid DNA sequences and was electroporated into mouse SV129 ES cells (clone CK35; a gift from C. Kress, Institut Pasteur, Paris, France). Transfected cells were selected with hygromycin 24 hours after electroporation. The DNA of 400 resistant ES cell clones was analyzed by Southern blotting using 2 probes, an internal AT_{1A} sequence probe (probe 1) and an external 3' fragment probe (probe 2). Digestion of the genomic DNA with SpeI resulted in a 4.8-kb band for the recombinant gene and a 9-kb band for the endogenous WT gene with probe 1. SacI digestion resulted in a 5-kb band for the recombinant gene and a 3-kb band for the endogenous gene recognized by probe 2 (Figure 1, A and B).

Two appropriate clones were identified by Southern blot (1 positive ES cell clone is shown in Figure 1B) and PCR (data not shown) and presented a normal karyotype. They were microinjected into C57BL/6 blastocysts, which were then implanted into pseudopregnant mice. Several chimeric animals from 2 different lines were able to transmit the transgene to their progeny. Heterozygous progeny was obtained by successive backcrosses to C57BL/6 females. Homozygous and heterozygous animals were obtained



Table 4
Echocardiographic assessment of cardiac phenotypes of AT_{1A}WT and AT_{1A}MUT mice

Age	5 mo		12 mo	
	AT _{1A} WT (n = 8)	AT _{1A} MUT (n = 8)	AT _{1A} WT (n = 11)	AT _{1A} MUT (n = 11)
HR (bpm)	550 ± 11	506 ± 13 ^A	563 ± 7	535 ± 12
LVEDD/BW	0.15 ± 0.01	0.17 ± 0.01 ^A	0.13 ± 0.005	0.15 ± 0.004
LV mass/BW (mg/g)	4.17 ± 0.29	4.97 ± 0.32	4.42 ± 0.16	4.41 ± 0.24
Ef (%)	80.0 ± 1.8	80.0 ± 0.5	82.0 ± 0.03	81.0 ± 2.1
Sa (cm/s)	3.08 ± 0.14	2.48 ± 0.12 ^A	2.96 ± 0.09	2.37 ± 0.11 ^A
Spw (cm/s)	3.44 ± 0.27	2.38 ± 0.16 ^A	3.09 ± 0.16	2.72 ± 0.19
IVRT (ms)	14.89 ± 0.35	17.2 ± 1.11 ^A	14.2 ± 0.66	18 ± 0.57 ^A
Ea (cm/s)	5.61 ± 0.23	4.99 ± 0.26	5.71 ± 0.26	4.35 ± 0.25 ^A
Epw (cm/s)	4.77 ± 0.38	3.87 ± 0.26 ^A	4.72 ± 0.22	3.95 ± 0.21 ^A
E/Ea	16.7 ± 0.8	17.9 ± 0.5	14.3 ± 0.7	19.5 ± 0.9 ^A

HR, heart rate; LVEDD/BW, LV end-diastolic diameter normalized to body weight; Ef, ejection fraction; Sa, maximal systolic velocity of the mitral annulus; Spw, maximal systolic velocity of the posterior wall; IVRT, isovolumic relaxation time; Ea, early diastolic mitral annular velocity; Epw, early diastolic motion velocity of the posterior wall; E/Ea, ratio of the maximal blood velocity of early LV inflow to the maximal velocity of early diastolic motion of the mitral annulus. ^AP < 0.05 compared with AT_{1A}WT.

gene) were used for acquisition and quantification of protein phosphorylation.

For basal STAT1, STAT3, and ERK1/2 phosphorylation in tissues, identical amounts of liver, kidney, and heart protein extracts of AT_{1A}WT and AT_{1A}MUT mice were analyzed using western blot. Anti-phospho and total protein antibodies were from Santa Cruz Biotechnology (p-ERK1/2, and STAT3), Millipore (STAT1 and p-STAT3), Cell Signaling Technology (p-STAT1), and Promega (ERK1/2).

BP measurements

Arterial systolic BP and heart rate were measured by a tail-cuff plethysmography method in trained conscious mice that had been placed in a warming restrainer (Phympex) as previously described (43). Measurements were repeated for 4 days after training, and approximately 10 consecutive inflation cycles were performed per day. Successful measurements were averaged to determine the per-

day BP for each mouse. For AT₁ blockade assay, candesartan (AstraZeneca) was added to drinking water at 10 mg/kg/d for 25 days. In another set of experiments, losartan (Teva Pharmaceutical Industries Ltd.) was added to drinking water at 30 mg/kg/d for 15 days and then at 150 mg/kg/d for 15 additional days. BP was measured as described above for the last 3 days of each treatment period.

without prenatal or perinatal lethality and have normal fertility. All offspring were genotyped using Southern blot analysis of tail biopsies with the external probe (probe 2) as shown in Figure 1C.

Mice were housed in colony cages with a 12-hour light/12-hour dark cycle in a temperature-controlled environment and had free access to water and a standard diet. Animal studies described here were performed by S. Billet with the help of M.A. Ventura (Agreement no. 7611, as approved by the French Department of Agriculture) in the animal facilities of Cochin Institute (Agreement no. DTPP.2007-66, from Prefecture de Police de Paris).

Pharmacological and signaling characterization of the AT_{1A}MUT mouse

AT_{1A} in AT_{1A}WT and AT_{1A}MUT mice was characterized using freshly isolated hepatocytes, the liver being an organ which expresses this receptor subtype exclusively and strongly (4). The hepatocytes were isolated using the collagenase method as previously described (41). Freshly isolated hepatocytes were then seeded on culture plates for the ERK1/2 phosphorylation assays or were used in suspension for cell membrane extraction in pharmacological experiments.

Saturation and competitive binding assays. Fifty micrograms of purified hepatocyte membranes were incubated with [¹²⁵I]Ang II with or without various amounts of competitive Ang II ligands, as previously described (42). Saturation studies were performed with 0.1–4 nM [¹²⁵I]Ang II. For competition binding assays, 0.5 nM of [¹²⁵I]Ang II and concentrations (10⁻¹¹ to 10⁻⁴ M) of different ligands were used. Each experiment was performed in triplicate. Binding data were analyzed by linear regression with the Prism Program (version 3.0; Graph Pad Software).

Protein phosphorylation analysis. Freshly isolated hepatocytes were seeded on collagen-coated plates at a density of 5 × 10⁵ cells in M199 medium as previously described (41). After cell attachment (2 hours at 37°C, 5% CO₂), cells were washed once with M199 medium and incubated for 3 hours at 37°C with fresh serum-free M199 medium for depletion. Then cells were stimulated at 37°C for 5 minutes with Ang II or Ang IV. ERK phosphorylation was analyzed by western blot as previously described (18) using either anti-phospho-ERK1/2 antibody (1/1,000; Cell Signaling Technology) or anti-ERK1/2 antibody (1/1,000; Millipore) and an enhanced chemiluminescence kit (SuperSignal West Pico; Pierce Biotechnology). ChemiGenius 2, GeneSnap (version 6.00), and GeneTools software (version 3.07.03) (Syn-

In vivo Ang II reactivity

Acute pressor response to Ang II was measured in anesthetized mice. Flexible plastic catheters were introduced into the femoral artery and in the jugular vein. The arterial catheter was connected to a pressure transducer and a Gould RS 3400 polygraph, and the venous catheter was connected to a syringe for drug injection. The signal was amplified and recorded by a Biopac data acquisition system (MP100; Harvard Apparatus). After at least 30 minutes – necessary to stabilize BP and heart rate – bolus injections of increasing doses of Ang II (0.0001–30 μg/kg) or CGP42112A (0.015–5,000 μg/kg) were administered at 10-minute intervals. Dose response curves were established for the peak of the BP responses, the area under the curve from the time of injection to 8 minutes after injection, and the BP difference between 2 consecutive Ang II injections. Identical experiments were performed in mice after binephrectomy.

Biochemical measurements

Blood was collected by aorta puncture from anesthetized animals. Heparized blood samples were centrifuged at 3,000 g for 5 minutes, and plasma was collected and frozen.

For urinary determinations, mice were placed individually in metabolic cages for 3 days. Food and water intake and diuresis were measured every day.

Creatinine, urea, protein, Na⁺, and K⁺ were determined in plasma and urine using an Olympus multiparametric autoanalyzer. Hemoglobin, red blood cell concentration, and hematocrit were determined using a Beckman Coulter MAXM automatic analyzer. Plasma and urine osmolalities were measured by Roebbling automatic microosmometer.

Plasma renin concentrations were measured by an indirect enzymatic assay, which determined by RIA the Ang I production of the plasma in the presence of an excess of the substrate angiotensinogen, as previously described (44). Plasma and urine aldosterone concentrations were determined by RIA assay as previously described (45). Immunoreactive angio-



tensin was measured in plasma by RIA as previously described (46). This assay measures Ang II, Ang III, and Ang IV together.

Echocardiographic analysis

Echocardiography was performed on lightly anesthetized (1% isoflurane in oxygen; Abbot) 5- and 12-month-old mice, as previously described (47). Briefly, left ventricle dimensions and pulse-wave tissue Doppler velocity measurements of the posterior wall (Spw) were obtained from the parasternal long-axis view. Left ventricle inflow and outflow pulse-wave Doppler velocities, as well as pulse-wave tissue Doppler of the mitral annulus (Ea and Sa) were obtained from apical 5-chamber view.

Molecular and cellular analyses in Ang II target tissues

Mice were killed and organs (including heart, aorta, kidney, adrenal gland, and liver) were collected. The organs were briefly rinsed with 0.9% saline to remove blood, blotted dry, and weighed.

For immunoperoxidase staining and in situ hybridization, organs were fixed in 4% buffered paraformaldehyde and embedded in paraffin. Sections mounted for histology were hybridized with cRNA ³⁵S-labeled probes as previously reported (48). Extracellular matrix was stained using Sirius red as described in ref. 49. Samples were examined by optical microscopy.

Morphometric analysis of arteries. Multiple nonadjacent kidney sections from AT_{1A}WT and AT_{1A}MUT mice were immunohistochemically labeled with an anti-smooth muscle α -actin antibody. For each α -actin-positive artery, the surface of the media (S) and the longest external diameter (L) were measured as previously described (50). Small arteries with L values between 10 μ m and 150 μ m were selected. The S/L ratio was used as an index of arterial wall thickness. This ratio was measured for at least 20 different renal arteries for each mouse and was compared between AT_{1A}WT and AT_{1A}MUT mice.

In situ hybridization. Riboprobes were obtained by in vitro transcription of cloned cDNA for human renin, rat angiotensinogen, mouse ACE, rat AT₁, and AT₂, and a specific probe of the mouse CYP11B2 (nucleotides 825 to 901 of NM009991). After rehydration, microwave heating, and proteinase K digestion, the paraffin-embedded sections were hybridized with 10⁴ cpm/ μ l of ³⁵S-labeled antisense or sense riboprobe in 30 to 50 μ l of hybridization mixture at 50°C for 16 hours. Samples were washed and then digested with RNase A (20 μ g/ml) as previously described (48). The slides were dipped into NTB2 liquid emulsion (Kodak) and stored for 1 to 4 weeks at 4°C in the dark until photographic processing. At the end of the procedure, the slides were examined under a microscope, photographed, and stained with toluidine blue.

Quantitative RT-PCR. Quantitative RT-PCR was used to compare the expression of different genes (*Agtr1a*, *Agtr1b*, *Agtr2*, *Nppa*, *Nppb*, *Col1a1*, and *serpine1*) in the AT_{1A}WT and AT_{1A}MUT mice using the LightCycler technology (Roche Applied Science). The common reference was the cyclophilin gene. Several tissues were analyzed, including liver, heart, kidney, adrenal, and aorta. Total RNA was extracted from these tissues using TRIzol reagents according to the manufacturer’s instructions (Invitrogen), and reverse transcription was performed with the SuperScript II Reverse Transcriptase kit (Invitrogen). All other procedures involving the LightCycler were performed according to manufacturer’s instructions (Roche Applied Science).

Statistics

Values are expressed as mean \pm SEM. Groups were compared by ANOVA, 2-tailed Student’s *t* test, or a nonparametric test, depending on the nature of the comparison. InStat version 2.01 (GraphPad Software) or StatView (version 5) softwares were used. For tail-cuff BP and heart rate measurements, grouping factors were taken into account by using the multiple comparisons procedure. A *P* value of 0.05 or less was considered significant.

Acknowledgments

We are grateful to M. Brand for arterial measurements, F. Letourneur for DNA sequencing, and D. Laude for statistical analysis. We also thank J. Ménard for his insightful comments about the manuscript and J.B. Michel for helpful discussions and comments. This work was supported by INSERM, CNRS, and Université Paris Descartes and by grants from Agence Nationale de la Recherche (ANR) Pathophysiology Programme of Human Diseases, Comité de Paris de la Ligue Nationale Contre le Cancer, Association pour la Recherche sur le Cancer (ARC), Fondation de France, Société Française d’Hypertension Artérielle (SFHTA), and MSD-Chibret.

Received for publication April 6, 2006, and accepted in revised form April 24, 2007.

Address correspondence to: Eric Clauser, Département d’Endocrinologie, Métabolisme et Cancer, Institut Cochin, Faculté de Médecine Paris Descartes, 24 rue du Faubourg Saint Jacques, 75014 Paris, France. Phone: 33-153-73-27-50; Fax: 33-153-73-27-51; E-mail: clauser@cochin.inserm.fr.

1. Clauser, E., et al. 1995. Molecular structure and mechanisms of action of mammalian angiotensin II receptors. *Curr. Opin. Endocrinol. Diabetes.* **2**:404–411.
2. Sandberg, K., Ji, H., Clark, A.J., Shapira, H., and Catt, K.J. 1992. Cloning and expression of a novel angiotensin II receptor subtype. *J. Biol. Chem.* **267**:9455–9458.
3. Murphy, T.J., Alexander, R.W., Griendling, K.K., Runge, M.S., and Bernstein, K.E. 1991. Isolation of a cDNA encoding the vascular type-1 angiotensin II receptor. *Nature.* **351**:233–236.
4. Llorens-Cortes, C., Greenberg, B., Huang, H., and Corvol, P. 1994. Tissue expression and regulation of type 1 angiotensin II receptor subtypes by quantitative reverse transcriptase-polymerase chain reaction analysis. *Hypertension.* **24**:538–548.
5. Sugaya, T., et al. 1995. Angiotensin II type 1a receptor-deficient mice with hypotension and hyperreninemia. *J. Biol. Chem.* **270**:18719–18722.
6. Ito, M., et al. 1995. Regulation of blood pressure by the type 1A angiotensin II receptor gene. *Proc. Natl. Acad. Sci. U. S. A.* **92**:3521–3525.
7. Chen, X., et al. 1997. Targeting deletion of angiotensin type 1B receptor gene in the mouse. *Am. J. Physiol.* **272**:F299–F304.
8. Le, T.H., et al. 2003. Physiological impact of increased expression of the AT1 angiotensin receptor. *Hypertension.* **42**:507–514.
9. Agarwal, A., Williams, G.H., and Fisher, N.D. 2005. Genetics of human hypertension. *Trends Endocrinol. Metab.* **16**:127–133.
10. Cotecchia, S., Exum, S., Caron, M.G., and Lefkowitz, R.J. 1990. Regions of the alpha 1-adrenergic receptor involved in coupling to phosphatidylinositol hydrolysis and enhanced sensitivity of biological function. *Proc. Natl. Acad. Sci. U. S. A.* **87**:2896–2900.
11. Schipani, E., Kruse, K., and Juppner, H. 1995. A constitutively active mutant PTH-PTHrP receptor in Jansen-type metaphyseal chondrodysplasia. *Science.* **268**:98–100.
12. Parma, J., et al. 1993. Somatic mutations in the thyrotropin receptor gene cause hyperfunctioning thyroid adenomas. *Nature.* **365**:649–651.
13. Davies, E., Bonnardeaux, A., Plouin, P.F., Corvol, P., and Clauser, E. 1997. Somatic mutations of the angiotensin II (AT1) receptor gene are not present in aldosterone-producing adenoma. *J. Clin. Endocrinol. Metab.* **82**:611–615.
14. Sachse, R., et al. 1997. Absence of angiotensin II type 1 receptor gene mutations in human adrenal tumors. *Eur. J. Endocrinol.* **137**:262–266.
15. Parnot, C., et al. 2000. Systematic identification of mutations that constitutively activate the angiotensin II type 1A receptor by screening a randomly mutated cDNA library with an original pharmacological bioassay. *Proc. Natl. Acad. Sci. U. S. A.* **97**:7615–7620.
16. Miserey-Lenkei, S., Parnot, C., Bardin, S., Corvol, P., and Clauser, E. 2002. Constitutive internalization of constitutively active angiotensin II AT(1A) receptor mutants is blocked by inverse agonists. *J. Biol. Chem.* **277**:5891–5901.
17. Conchon, S., Peltier, N., Corvol, P., and Clauser, E. 1998. A noninternalized nondesensitized truncated AT1A receptor transduces an amplified ANG II signal. *Am. J. Physiol.* **274**:E336–E345.
18. Billet, S., Bardin, S., Tacine, R., Clauser, E., and Conchon, S. 2006. The AT1A receptor “gain-of-function” mutant N111S/delta329 is both consti-



- tutively active and hyperreactive to angiotensin II. *Am. J. Physiol. Endocrinol. Metab.* **290**:E840–E848.
19. Le, M.T., et al. 2003. Peptide and nonpeptide antagonist interaction with constitutively active human AT1 receptors. *Biochem. Pharmacol.* **65**:1329–1338.
20. Clark, A.F., et al. 1997. Renin-1 is essential for normal renal juxtaglomerular cell granulation and macula densa morphology. *J. Biol. Chem.* **272**:18185–18190.
21. Esther, C.R., Jr., et al. 1996. Mice lacking angiotensin-converting enzyme have low blood pressure, renal pathology, and reduced male fertility. *Lab. Invest.* **74**:953–965.
22. Krege, J.H., et al. 1995. Male-female differences in fertility and blood pressure in ACE-deficient mice. *Nature.* **375**:146–148.
23. Sharp, M.G., et al. 1996. Targeted inactivation of the Ren-2 gene in mice. *Hypertension.* **28**:1126–1131.
24. Kim, H.S., et al. 1995. Genetic control of blood pressure and the angiotensinogen locus. *Proc. Natl. Acad. Sci. U. S. A.* **92**:2735–2739.
25. Ohkubo, H., et al. 1990. Generation of transgenic mice with elevated blood pressure by introduction of the rat renin and angiotensinogen genes. *Proc. Natl. Acad. Sci. U. S. A.* **87**:5153–5157.
26. Mullins, J.J., Peters, J., and Ganten, D. 1990. Fulminant hypertension in transgenic rats harbouring the mouse Ren-2 gene. *Nature.* **344**:541–544.
27. Oliverio, M.I., et al. 1998. Renal growth and development in mice lacking AT1A receptors for angiotensin II. *Am. J. Physiol.* **274**:F43–F50.
28. Ichiki, T., et al. 1995. Effects on blood pressure and exploratory behaviour of mice lacking angiotensin II type-2 receptor. *Nature.* **377**:748–750.
29. Hein, L., Barsh, G.S., Pratt, R.E., Dzau, V.J., and Kobilka, B.K. 1995. Behavioural and cardiovascular effects of disrupting the angiotensin II type-2 receptor in mice. *Nature.* **377**:744–747.
30. Samama, P., Bond, R.A., Rockman, H.A., Milano, C.A., and Lefkowitz, R.J. 1997. Ligand-induced overexpression of a constitutively active beta2-adrenergic receptor: pharmacological creation of a phenotype in transgenic mice. *Proc. Natl. Acad. Sci. U. S. A.* **94**:137–141.
31. Milano, C.A., et al. 1994. Myocardial expression of a constitutively active alpha 1B-adrenergic receptor in transgenic mice induces cardiac hypertrophy. *Proc. Natl. Acad. Sci. U. S. A.* **91**:10109–10113.
32. Hata, J.A., Williams, M.L., and Koch, W.J. 2004. Genetic manipulation of myocardial beta-adrenergic receptor activation and desensitization. *J. Mol. Cell. Cardiol.* **37**:11–21.
33. Audoly, L.P., Oliverio, M.I., and Coffman, T.M. 2000. Insights into the functions of type 1 (AT1) angiotensin II receptors provided by gene targeting. *Trends Endocrinol. Metab.* **11**:263–269.
34. Gordon, R.D., Laragh, J.H., and Funder, J.W. 2005. Low renin hypertensive states: perspectives, unsolved problems, future research. *Trends Endocrinol. Metab.* **16**:108–113.
35. Crowley, S.D., et al. 2005. Distinct roles for the kidney and systemic tissues in blood pressure regulation by the renin-angiotensin system. *J. Clin. Invest.* **115**:1092–1099. doi:10.1172/JCI200523378.
36. Oliverio, M.I., et al. 2000. Abnormal water metabolism in mice lacking the type 1A receptor for ANG II. *Am. J. Physiol. Renal Physiol.* **278**:F75–F82.
37. Hein, L., et al. 1997. Overexpression of angiotensin AT1 receptor transgene in the mouse myocardium produces a lethal phenotype associated with myocyte hyperplasia and heart block. *Proc. Natl. Acad. Sci. U. S. A.* **94**:6391–6396.
38. Paradis, P., Dali-Youcef, N., Paradis, F.W., Thibault, G., and Nemer, M. 2000. Overexpression of angiotensin II type I receptor in cardiomyocytes induces cardiac hypertrophy and remodeling. *Proc. Natl. Acad. Sci. U. S. A.* **97**:931–936.
39. Zhai, P., et al. 2005. Cardiac-specific overexpression of AT1 receptor mutant lacking Gαq/Gαi coupling causes hypertrophy and bradycardia in transgenic mice. *J. Clin. Invest.* **115**:3045–3056. doi:10.1172/JCI25330.
40. Matsusaka, T., Katori, H., Inagami, T., Fogo, A., and Ichikawa, I. 1999. Communication between myocytes and fibroblasts in cardiac remodeling in angiotensin chimeric mice. *J. Clin. Invest.* **103**:1451–1458.
41. Dentin, R., et al. 2005. Polyunsaturated fatty acids suppress glycolytic and lipogenic genes through the inhibition of ChREBP nuclear protein translocation. *J. Clin. Invest.* **115**:2843–2854. doi:10.1172/JCI25256.
42. Bihoreau, C., et al. 1993. Mutation of Asp74 of the rat angiotensin II receptor confers changes in antagonist affinities and abolishes G-protein coupling. *Proc. Natl. Acad. Sci. U. S. A.* **90**:5133–5137.
43. Le Menuet, D., et al. 2001. Alteration of cardiac and renal functions in transgenic mice overexpressing human mineralocorticoid receptor. *J. Biol. Chem.* **276**:38911–38920.
44. Menard, J., and Catt, K.J. 1972. Measurement of renin activity, concentration and substrate in rat plasma by radioimmunoassay of angiotensin I. *Endocrinology.* **90**:422–430.
45. Pham-Huu-Trung, M.T., and Corvol, P. 1974. A direct determination of plasma aldosterone. *Steroids.* **24**:587–598.
46. Lachurie, M.L., Azizi, M., Guyene, T.T., Alhenc-Gelas, F., and Menard, J. 1995. Angiotensin-converting enzyme gene polymorphism has no influence on the circulating renin-angiotensin-aldosterone system or blood pressure in normotensive subjects. *Circulation.* **91**:2933–2942.
47. Parlakian, A., et al. 2005. Temporally controlled onset of dilated cardiomyopathy through disruption of the SRF gene in adult heart. *Circulation.* **112**:2930–2939.
48. Sibony, M., Commo, F., Callard, P., and Gasc, J.M. 1995. Enhancement of mRNA in situ hybridization signal by microwave heating. *Lab. Invest.* **73**:586–591.
49. Nicoletti, A., et al. 1995. Left ventricular fibrosis in renovascular hypertensive rats. Effect of losartan and spironolactone. *Hypertension.* **26**:101–111.
50. Brand, M., et al. 2006. Angiotensinogen modulates renal vasculature growth. *Hypertension.* **47**:1067–1074.